Numerical Model Calibration for Simulating Coal Pillars, Gob and Overburden Response

Essie Esterhuizen, Senior Service Fellow
Chris Mark, Principal Reserach Engineer, Mining Engineer
Michael M. Murphy, Research Engineer, Mining Engineer
Ground Control Branch
NIOSH, Office of Mine Safety and Health Research
Pittsburgh, PA

ABSTRACT

The design of underground coal mines requires a clear understanding of the overburden response, the loading of pillars, the loading of the gob, the pillar failure process, and the ultimate load carried by partly or fully yielding pillars. Very few high-quality stress measurements of yielding pillars and gob loading have been made in full extraction mining. Well-calibrated numerical models can assist in providing a better understanding of the load and failure processes, provided the coal, the overburden, and the gob are all modeled with sufficient realism. A program of numerical model calibration and validation was carried out using FLAC3D.[1] The models were calibrated against observed and measured performance of coal pillars and the overburden in operating mines to provide a basic set of input parameters that can be used to provide a realistic first estimate of expected ground response and pillar loading. Input parameters for modeling coal pillar response were based on data from triaxial testing on coal samples, combined with both matching the depth of failure in the coal ribs to observations as well as matching the peak pillar resistance to an empirical equation. The models were calibrated against strong roof and floor case histories in which the pillar strength is governed by failure and yielding of the coal within the pillar and the surrounding strata only had a limited impact on pillar strength. Input parameters for the overburden were determined from a large database of laboratory tests and model calibration against maximum subsidence and subsidence curvature. Further overburden calibration was carried out by matching stresses in the mining horizon to field measurements. Three examples of the application of the calibrated dataset and modeling methodology to field measurements are presented. The results show that a reasonable estimate of the in-seam stress distribution and overburden response can be obtained for both strong and weak overburden scenarios at various depths of cover.

INTRODUCTION

The planning and design of coal mine excavations requires reliable estimates of the expected strength and loading of the mine structures to achieve global stability. Empirical methods are widely used to estimate the strength and loading of coal pillars and have been incorporated into pillar design procedures, such as Analysis of Longwall Pillar Stability (ALPS) (Mark, 1987) and Analysis of Retreat Mining Pillar Stability (ARMPS) (Mark and Chase, 1997), that are widely used in the United States. Numerical models are finding increasing application as a tool for underground mine design because of their versatility and the ever increasing computational power available to mine designers. A prerequisite for the application of numerical models is the calibration of the models against observed rock mass response (Hoek et al., 1990; Skiles and Stricklin, 2009). The calibration process may include comparison of model results to measured stress and deformation and modifying the input parameters in a systematic manner to achieve a satisfactory agreement between the model results and measurements. Once models have been calibrated, they can be applied to evaluating similar mining layouts in similar geological conditions.

Models that correctly simulate the basic mechanics of rock failure and deformation are required to improve the prediction of the larger scale rock mass response to mining excavations. However, knowing the likely deformations and extent of rock fracturing does not fully predict the actual mining conditions. Empirical relationships need to be established between model outputs and the serviceability of the proposed mining excavations. Such relationships need to include both model outputs and significant geological structures that impact excavation stability. For example, Wang and Heasley (2005) describe a system that allows composite hazard maps to be developed in which various geological data and numerical model outputs can be combined into a single index.

During the planning stages of a mine or a new section of a mine, data on local geological structures and variations of the bedded sequence can be limited. Planning is typically based on the expected "average" conditions. Modifications to the mining plan are made if hazardous conditions are exposed during development. Numerical models can provide additional insight into the expected response of the "average" rock mass, but the reliability of the prediction is not better than the available geotechnical data.

When developing a numerical model, one of the first challenges is to identify appropriate input parameters for modeling the

1 Mention of any company name or product does not constitute endorsement by the National Institute for Occupational Safety and Health.

rock mass. The large-scale strength of the rock mass needs to be known as well as the initial loading conditions. Establishing appropriate values for rock mass strength can be a challenge because laboratory-determined test results do not necessarily represent the properties of the large-scale rock mass. Methods of relating laboratory tests to the large-scale rock mass strength have been developed (Hoek and Brown, 1997) and can be used as a first estimate. However, these relationships are more appropriate for a relatively homogeneous, jointed rock mass, rather than the strongly bedded and highly variable rock layering that is found in coal mine strata. The initial stress conditions in coal strata can also be more complex than in more homogeneous rock masses. In the eastern and midwestern United States, the in situ horizontal stress appears to be caused by current-day tectonic loading, (Zoback and Zoback, 1989; Dolinar, 2003; Mark and Gadde, 2008), resulting in horizontal stress that is greater in stiffer rock strata. The resulting variation in horizontal stress should be included in numerical models. Further issues exist when attempting to model the gob response. Little is known about the extent of caved rock above the mining horizon and the properties of the fully caved and partially caved material. Nevertheless, numerical models have found wide acceptance in coal mine design, in spite of the difficulties and challenges associated with model development and calibration.

This paper addresses the need for a basic set of model parameters to provide a first estimate of the expected rock mass response in U.S. coal mines. The models were calibrated against published case histories of in situ monitoring of the rock mass response to coal mining as well as laboratory testing of coal, intact rock, and gob materials. This paper does not, however, provide relationships between model outputs and excavation serviceability indices.

The modeling software used in this paper is FLAC3D (Anon., 2007). The model parameters will be useful as initial estimates when using other modeling techniques, but each technique should be calibrated independently.

PILLAR STRENGTH MODELING

The strength of pillars is affected by the properties of the coal within the pillars, the contact between the coal and the surrounding rock mass, and the response of the surrounding rock mass to the pillar stress. Therefore, the pillar-roof-floor system should be considered as a unit when assessing pillar strength.

Strength of the Coal

The scale dependence of rock strength, particularly coal, has received much attention in rock engineering literature (Hoek and Brown, 1980; Bieniawski, 1968). Coal is one of the few rock materials that has been extensively tested at various scales and the results indicate that its strength reduces as the sample size increases. For modeling purposes, the coal strength as well as the residual strength and the rate of strength decay need to be known.

The Hoek-Brown constitutive model that is available in FLAC3D was used to model the coal strength. The peak strength is assumed to follow the Hoek-Brown rock mass strength criterion (Hoek et al., 2002) and yield is modeled based on strain softening and non-associated plastic flow rules. The Hoek-Brown criterion describes a non-linear relationship between confinement and stress, and can be written as follows, in its general form:

$$\sigma_1 = \sigma_3 + \sigma_c \left(\frac{m\sigma_3}{\sigma_c} + s\right)^a \quad (1)$$

where σ_1 and σ_3 are the effective principal stresses; σ_c is the strength of the intact rock; and m, s, and a are empirically derived parameters. The parameters can be determined by laboratory testing of small samples of rock. However, obtaining the parameters for the large-scale rock mass cannot be practically done by direct testing. Methods for estimating these parameters from rock mass classification data and small-scale laboratory tests have been proposed (Hoek and Brown, 1997).

To obtain a set of realistic coal strength parameters for the Hoek-Brown criterion, the strength of laboratory-scale coal samples was first considered. Unpublished triaxial test data available to the authors, supplemented by published data (Atkinson and Ko, 1977; Morsy and Peng, 2001; Newman and Hoelle, 1993), were used to determine an initial set of parameters describing laboratory coal strength. There was a considerable scatter in the results, and each data set was assessed individually. The s-parameter was set to 1.0, which represents intact rock material, and the a-parameter was set at either 0.50 or 0.65, depending on which value provided the best fit. The resulting m-parameter for the intact coal (m_i) was determined for each data set. The resulting m_i-values ranged between a low of 5.0 and a high value of 17.6, and the uniaxial compressive strength (UCS) of the coal varied between 16 MPa and 40 MPa (2,321 and 5,802 psi).

The next step was to modify the m- and s-parameters so that they would be representative of a large-scale (1-m (3.3-ft) edge) coal sample. The literature contains several approaches to estimate this value, since it is impractical to determine it by direct testing. For example, Gadde et al. (2007) estimated the large-scale m-parameter for coal through rock classification considerations. Barron and Yang (1992) showed that the coal type and rank result in an m-parameter variation and proposed that the large-scale m-parameter can be estimated from the coal rank number. Medhurst and Brown (1988) conducted triaxial strength tests on laboratory samples with diameters of 61 mm (2.4 in) up to 300 mm (12 in) and extrapolated the results to large-scale coal. They assumed that the 61-mm (2.4 in) samples represent "intact" coal and the larger samples were considered to represent increasingly fractured coal as the number of cleats and flaws in the samples increased. The results of the study showed that the m-value decreases with sample size. For medium rank, mid-brightness coal samples, they found that setting the a-parameter to 0.65 gives the best fit to the test results and the following relationship can be used to estimate the in situ m-value for large-scale coal:

$$\frac{m}{m_i} = 0.15 \quad (2)$$

Using the above relationship the *m*-parameter for U.S. coal can be calculated. Based on the review of triaxial tests on U.S. coal samples, the m_i-parameter for "average" U.S. coal was calculated to be 9.8, which is the average of the laboratory derived values. The *m*-parameter for the large-scale coal can then be calculated to be 1.47, using Equation 2. This value of the *m*-parameter was used in all the pillar models described in this paper.

Further parameters that are required for modeling large-scale coal are the *s*-parameter of the large-scale coal, the residual *m*- and *s*-parameters, and the rate of strain softening from the peak to the residual strength. These parameters have not been determined in the laboratory due to practical problems with preparing, handling, and crushing such large blocks of material. An alternative approach may be to use rock classification methods to estimate the *s*-parameter and the residual values of *m* and *s*. However, rock classification methods are poorly suited to classifying coal material. In addition, the relationships between classification values and the Hoek-Brown parameters are not necessarily valid for coal materials. Therefore, the final estimates of the unknown parameters were obtained through numerical model calibration against empirically derived pillar strength equations, observed failure of coal in pillar ribs, and measurements of stress distributions in coal pillars.

Numerical Model Testing to Obtain Unknown Parameters

The unknown strength parameters of the coal were determined by creating numerical models of coal pillars and subjecting them to increasing loads while monitoring their stress-strain response. The pillar response was compared to empirical strength equations and to field monitoring data and the unknown parameters were varied until satisfactory agreement was obtained between model response and observed pillar performance. At all times, the reasonableness of the inputs was considered against measured values.

Numerical models were created in which a portion of the roof strata, the coal pillar, and the floor strata were simulated. Pillars with width-to-height ratios of 3, 4, 6, 8 and 10 were modeled. Interface elements were used to model the contacts between the coal and the surrounding rocks. The surrounding rocks were elastic having a Young's modulus of 20 GPa (2,901 ksi) and Poisson's ratio of 0.25. Figure 1 shows a pillar model with the coal, roof, and floor strata included, only a quarter of a full pillar was modeled because of symmetry.

The model pillars were loaded by gradual compression in the vertical direction. The rate of compression was controlled so that the unbalanced forces in the model remained within pre-defined limits. As the stress in the model increased, failure and deformation of the coal was allowed to occur based on the defined strength properties and assumed unknown parameters. The model pillars were tested up to their peak strength and were allowed to yield to a residual value. Some of the wider pillars displayed strain hardening characteristics and the tests were typically stopped when the model deformation became excessive.

Bieniawski's (1992) empirical pillar strength equation was used for comparing the peak strength of the numerical models to actual pillar strength. The comparisons were carried out for pillars with width-to-height ratios of 3.0 to 8.0. Beyond a width-to-height ratio of 8.0 the empirical data are sparse. The large-scale coal strength

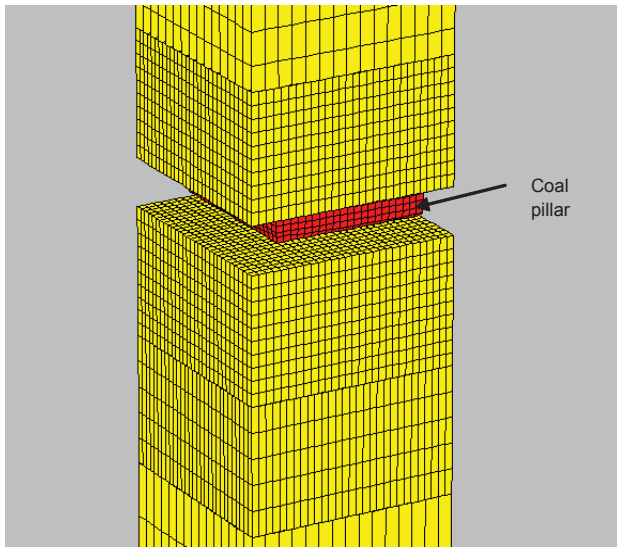

Figure 1. Example of a three dimensional model of a coal pillar and the surrounding roof and floor strata.

used in the Bieniawski equation was set at 6.2 MPa (899 psi) being representative of the typical coal strength in U.S. coal mines, after Mark and Chase (1997).

Field monitoring data in the form of stress measurements in pillars adjacent to longwall panels were used to verify that the extent of coal failure and the stress gradient at the edge of the pillars were acceptable. The calibration of the models against coal rib failure was carried out by comparing the model results to a series of pillar stress measurements from field study sites in the U.S. (Iannacchione, 1990a; Campoli et al., 1990; Koehler et al., 1996; Oram, 1996), shown in Figure 2. Vertical stress values in excess of 80 MPa (11,603 psi) were measured within the coal ribs at some of the sites. The depth of coal yield can be seen to extend about 5 m into the pillar where these peak stress values were measured. The figure also shows a collection of stress profiles determined by the numerical models, after final calibration of the coal properties. It can be seen that the peak stress in the model profiles follow a similar path as the measured results. For a peak stress of about 80 MPa (11,603 psi), the model shows the peak located at about 5 m (16 ft) into the pillar, which falls within the range of field results. It was concluded that the pillar models were satisfactory and were producing realistic peak strength values at the edges of pillars and depths of failure into the coal ribs.

Sensitivity studies of the effect of the interface properties showed, similar to the experience of other researchers (Gale, 1999; Iannacchione, 1990b; Lu et al., 2008), that the interface properties can have a significant effect on the strength of a pillar. However, if a similar stress gradient is desired at the edge of the pillar, as measured in underground trials, a friction angle of about 25° is required, with a nominal interface cohesion value of 0.1 MPa (14.5 psi). The friction angle of 25° is lower than the internal friction angle of most coal types and seems to be a reasonable value to represent a typical coal-rock interface.

After conducting many combinations of inputs, and always evaluating the assumptions for reasonableness and the outcomes

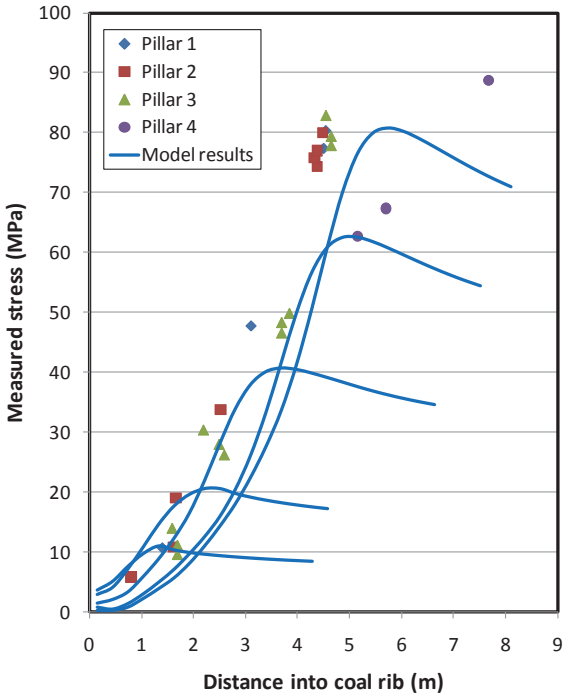

Figure 2. Stress at the edge of coal pillars subject to increased loading. Solid lines indicate model results of the stress profile at the edge of a W:H = 16 pillar at various loading stages. Symbols indicate field measurements at the edges of four longwall chain pillars.

against empirical results, the following set of input parameters was found to be satisfactory for modeling coal pillars based on the requirements of matching the Bieniawski strength equation and achieving similar depths of failure and stress gradients as observed in the field:

UCS (lab scale)	= 20 MPa (2,901 psi)
Young's modulus	= 3 GPa (435 ksi)
Poisson's ratio	= 0.25
m-value	= 1.47
s-value	= 0.07
m-residual	= 1.0
s-residual	= 0.001
Interface friction angle	= 25°
Interface cohesion	= 0.1 MPa (14.5 psi)
Interface tensile strength	= 0.0
Interface normal stiffness	= 100.0 GPa/m (14,504 ksi/m)
Interface shear stiffness	= 50 GPa/m (7,252 ksi/m)

The strength decrease of the coal from the peak to a residual value was allowed to take place over a plastic strain value of 0.04 for element sizes in the range of 0.30 to 0.33 m (1 to 1.1 ft). This value is affected by the element size used in the models, and needs to be adjusted if models are created using a significantly different element size. The FLAC3D software also has a dilation parameter that is used in the implementation of the Hoek-Brown criterion. This parameter was set to zero, mainly because non-zero values appeared to cause large geometric distortions of the yielding elements which were considered to be excessive. It is recognized that the final set of inputs is not unique, and it is possible that a different combination of input values can equally satisfy the empirical data.

Resulting Model Pillar Strength and Stress-Strain Response

Figure 3 shows the resulting stress-strain curves obtained from the pillar models. It can be seen that when the width-to-height ratio is 6.0 and below, the pillars exhibit a clear peak strength followed by strain softening behavior as the pillars continue to be compressed. However, for the width-to-height ratios of 8.0 and 10.0 the pillars do not display strain softening behavior, but become strain hardening. This type of behavior has been observed in laboratory tests on coal samples (Das, 1986) and is predicted by some pillar strength theories (Wilson, 1972; Salamon and Wagner, 1985).

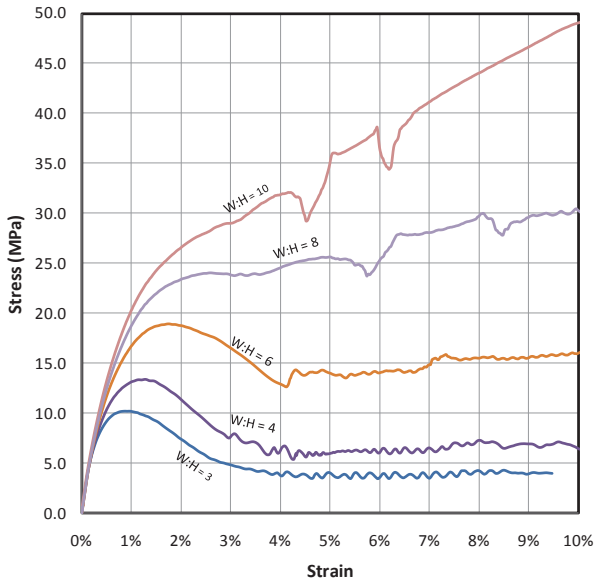

Figure 3. Stress-strain curves obtained from calibrated numerical models of pillars with width-to-height ratios of 3.0 to 10.0.

The peak pillar resistance produced by the numerical models is compared to the Bieniawski pillar strength equation up to a width-to-height ratio of 8.0 in Figure 4. The results show that satisfactory agreement has been achieved between the model results and the empirical equation, which was the target of the model calibration exercise.

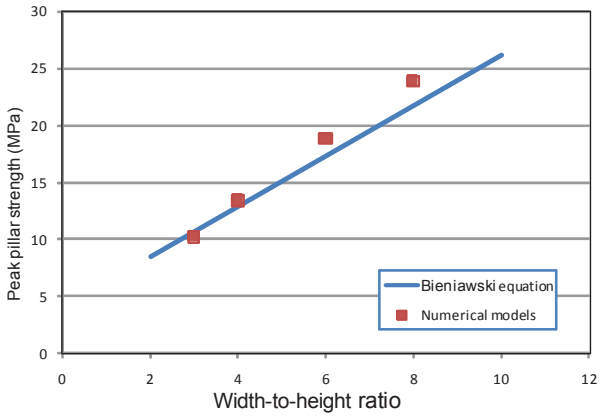

Figure 4. Pillar strength results obtained by numerical models after calibrating the models to the empirical pillar strength equation of Bieniawski (1989).

The Effect of Weak Surrounding Rocks

The above results were all obtained using models of coal that is contained between elastic roof and floor strata. The elastic material was not allowed to fail in the models. A number of analyses were carried out to evaluate the impact of weak and moderate strength roof and floor rocks on pillar strength, which showed that the peak pillar strength will be reduced if bedding slip occurs in the roof or floor. Other issues also arose, such as punching of the pillar core into the surrounding strata and pillar weakening if the roof collapses between the pillars. These phenomena have been observed in the field and can be analyzed using foundation engineering principles or numerical models (Chugh and Pytel, 1992; Gadde, 2009). Pillar design issues related to weak roof and floor strata fall beyond the scope of this paper. The results shown here assume that the pillar strength is governed by failure and yielding of the coal within the pillar and the surrounding strata have only a limited impact on the strength.

GOB RESPONSE MODELING

When modeling full extraction mining, such as longwall or pillar extraction, it is necessary to realistically simulate the gob (caved rock) in the mined out areas. The characteristics of the gob are difficult to measure in the field because of the large displacements that occur and fragmented nature of the caved rocks. Attempts have been made to locate load cells within the gob and measurements have been made in the floor strata below the gob (Iannacchione, 1990b). Laboratory tests on rock fragments have also provided valuable insight into the compaction behavior of fragmented gob materials (Pappas and Mark, 1993).

Gob Characteristics

The gob is usually subdivided into two zones: a lower, fully caved zone and an upper fractured zone (Peng and Chiang, 1984). The fully caved zone can be expected to extend vertically to about 2 to 3 times the mining height and behaves as a granulated material with a relatively high void ratio. The rock in the fractured zone has a relatively low void ratio but the overall strength is reduced owing to the presence of fracturing associated with the passage of the longwall panel face stress abutment.

Laboratory tests on coal measure shale and sandstone fragments showed that the stress-strain response of confined gob material follows an exponential hardening curve (Pappas and Mark, 1993). The tests were carried out on rock fragments that resembled a fully caved gob, having void ratios in the region of 30% to 40%. It was found that the stronger sandstone gob material had a stiffer response than the weaker shale material, as one would expect. A hyperbolic equation after Salamon (1990) was found to adequately represent the gob stress-strain behavior, which can be expressed as follows:

$$\sigma = \frac{a \times \varepsilon}{b - \varepsilon} \tag{3}$$

where a and b are empirically derived parameters and ε is the vertical strain. The b-parameter is related to the void ratio and the a-parameter is the gob stress when the strain is equal to $b/2$. For shale gob, the laboratory tests (Pappas and Mark, 1993) showed that a = 7.65 MPa (1,110 psi) and b = 0.442, and for sandstone gob, a = 13.03 MPa (1,890 psi) and b = 0.427.

Modeling Gob as a Strain Hardening Material

Gob modeling can follow two approaches. In the first approach, the intent may be to study roof fracturing, caving and gob development in response to mining. In this approach, it is necessary to explicitly model the gob formation process so that variations in geology and loading conditions can be studied. A second approach may be modeling of the effect of the gob on the surrounding coal mine entries and pillars. In the second situation, the gob is implicitly modeled; that is, the effect of the gob is modeled accurately so that the load redistribution to the surrounding rock and coal is correct and the large-scale overburden deflection and subsidence is correct. This paper addresses the second scenario, in which rock fracture and gob development is not explicitly modeled, but the effect of the gob needs to be included in a model.

When using the FLAC3D software, it is possible to simulate the effects of the fully-caved gob as a strain-hardening, granulated material using “double-yield” elements. These elements can model the compaction of granulated materials under increased loading using a cap-plasticity criterion and have been successfully used to model gob compaction and response (Esterhuizen and Barczak, 2006). Alternatively, when a large-scale model is set up, equivalent gob elements can be created by simply following the gob response curve without attempting to simulate the complex material behavior that forms the response curve (Board and Damjanac, 2003; Esterhuizen and Mark, 2009).

All the model calibrations presented in this paper were done using equivalent gob elements that follow the hyperbolic stress-strain curves (Equation 3). The gob response to various depths of cover, mining geometries and overburden types was investigated.

OVERBURDEN RESPONSE MODELING

The deflection and potential subsidence or collapse of the overburden has a significant impact on the load redistribution around coal mine panels. When full extraction mining is carried out, the overburden will settle onto the gob and stress will be regenerated in the mined area. The amount of stress regeneration depends on the gob stiffness as well as the stiffness of the overburden. Subsidence is also directly affected by the overburden properties and the panel width-to-depth ratio. Strong overburden strata can form a stable arch over a mined panel, which can result in significantly higher stress in the unmined coal while reducing the gob stress and magnitude of subsidence. The overburden stiffness also determines how stresses will be distributed over the unmined coal. Stiff overburden can be expected to transfer stress over a greater lateral distance than softer strata. When modeling the overburden, the characteristics of the overburden materials must be captured as accurately as possible to reproduce the observed response. The accuracy of the overburden models can be verified against field measurements of subsidence and of stress magnitudes in the coal surrounding mined panels.

Modeling Bedded Strata

The bedded overburden rocks were modeled using the strain softening, ubiquitous joint elements available in the FLAC3D software. These elements consist of a strain softening Coulomb material that represents the rock matrix and planes of weakness representing the bedding. The orientation and strength of the planes of weakness can be defined separately from the matrix properties and can also exhibit strain softening behavior. These elements allow a reasonable approximation of the characteristics of bedded strata to be made.

For the purpose of model calibration, a suite of rock strengths and bedding types was created, which could be combined to model any rock type, from a strong limestone with no bedding weaknesses to a low strength shale or claystone with smooth bedding planes. The initial properties of the strata were based on extensive databases of rock properties available at NIOSH as well as published data (Zipf, 2007; Rusnak and Mark, 2000). The approach was to simulate the rock matrix without any bedding effects or "rock mass" effects. The matrix strength of the in-situ rocks was determined from the laboratory scale strength using the relationship suggested by Hoek and Brown (1980):

$$\sigma_c = \sigma_{c50}\left(\frac{50}{d}\right)^{0.18} \tag{4}$$

where σ_{c50} is the laboratory sample diameter in mm and d is the field-scale sample diameter in mm. Assuming the laboratory sample size is nominally 50 mm (2 in), the strength of a 1,000 mm (4 in) sample will be 0.58 times the laboratory sample size.

Initial Stress

The initial stresses in the models were defined to closely match the current understanding of stress in the coal measures in the United States. The pre-mining vertical stress is gravity driven and is determined by the depth of the overburden. The horizontal stress is also depth dependent, but there is a tectonic component that is caused by the movement of the North American plate (Zoback and Zoback, 1989; Dolinar, 2003; Mark and Gadde, 2008). According to current understanding, the tectonic component of the horizontal stress is higher in stiff strata than in softer strata (Dolinar, 2003). In the numerical models, the pre-mining horizontal stress is calculated in each layer of rock, depending on its modulus of elasticity. The following equations are used, after Mark and Gadde (2008), to calculate the maximum and minimum horizontal stress components in MPa units:

$$\sigma_{h1} = 1.2\sigma_v + 2.6 + 0.003E \tag{5}$$

$$\sigma_{h2} = 1.2\sigma_v + 0.0015E \tag{6}$$

where E is the elastic modulus of the rock and σ_v is the vertical overburden stress.

OVERBURDEN AND GOB MODEL CALIBRATION

Calibration of the models was carried out by simulating total extraction mining of panels at various depths of cover and with various excavation spans. The model results were compared to predicted and measured subsidence profiles and empirically determined stress distributions from published case studies from around the United States. Correct modeling of the subsidence profile helps to confirm that the large-scale stiffness and deformation properties of the overburden and gob are reasonable. During the calibration stage, many combinations of rock strength properties and geometric scenarios were tested. Ultimately it was found that a single set of overburden material properties and gob properties could be used to obtain satisfactory agreement between model results and field observations for modeling the large-scale rock mass response and pillar response around full extraction panels.

Overburden Properties

The rock strength, deformation properties, and bedding strength properties suggested for modeling large-scale coal measure rocks in the United States are presented in Table 1. These properties can be used for panel scale models, where a single element can include both intact rock and weak bedding planes. Element sizes in the overburden models typically varied between 5 and 10 m (16 and 33 ft). Figure 5 shows a typical large-scale model that was used in the calibration exercises; the models always extended up to the ground surface and rock layering was modeled down to approximately 5-m (16-ft) bed thicknesses. Model element thickness varied between about 5 and 10 m (16 and 33 ft) in the proximity of the coal seam and was sometimes larger when modeling thick beds near the ground surface.

The uniaxial compressive strength shown in Table 1 is the laboratory-scale strength, which was reduced by the 0.58 factor from Equation 4 to simulate the large-scale strength in the models. Strength reduction owing to strain softening was achieved by reducing the rock cohesion only; the friction component of the

Table1. Representative rock properties.

Rock type	Laboratory sample			In situ rock material			In situ bedding planes		
	UCS (MPa)	Elastic modulus (GPa)	Friction angle (deg)	Cohesion (MPa)	Tensile strength (MPa)	Dilation angle (deg)	Bedding friction angle (deg)	Bedding cohesion (MPa)	Bedding tensile strength (Mpa)
Limestone 1	140	40	42	18.93	8.12	10	32	9.47	6.50
Limestone 2	100	35	42	15.10	5.8	10	30	7.55	4.64
Limestone 3	80	30	40	13.39	4.64	10	28	6.70	3.71
Sandstone 1	120	40	42	16.23	6.96	11	30	8.11	5.57
Sandstone 2	100	40	40	13.52	5.8	12	30	6.76	4.64
Sandstone 3	80	35	37	12.08	4.64	13	27	6.04	0.46
Sandstone 4	60	35	35	9.06	3.48	14	25	4.53	0.35
Sandstone 5	40	30	30	6.70	2.32	15	20	3.35	0.23
Shale 1	80	25	32	14.78	4.64	16	10	2.96	0.46
Shale 2	60	20	30	12.18	3.48	17	7	2.44	0.35
Shale 3	40	15	25	8.90	2.32	18	7	1.78	0.23
Shale 4	30	10	20	7.30	1.74	19	7	0.50	0.17
Shale 5	20	10	20	4.87	1.16	20	5	0.30	0.12
Shale 6	10	5	20	2.66	0.58	21	5	0.20	0.06
Shale 7	5	4	20	1.35	0.29	22	5	0.10	0.03

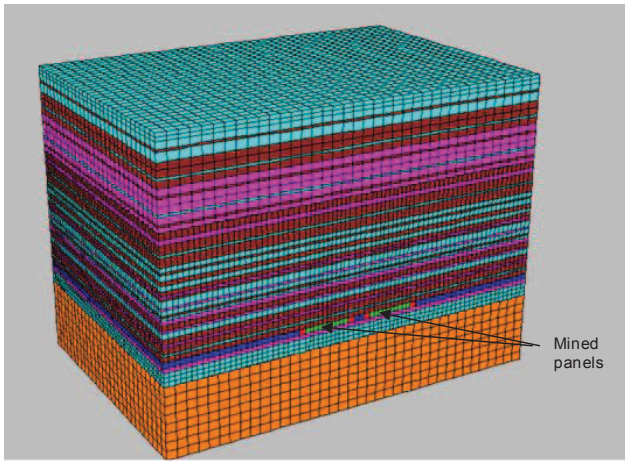

Figure 5. Example of a numerical model used to evaluate gob and overburden response. Layering represents different lithologies modeled. Gob is shown in green and unmined coal in dark blue.

strength was not altered. The Poisson's ratio was set at 0.25 and tensile strength set to 10% of the large-scale rock compressive strength. Bedding tensile strength was set at 10% of the large-scale rock tensile strength. The bedding friction angles may seem to be relatively low compared to small-scale laboratory test results. However, the presence of weak clayey materials, especially in shale beds, can have a significant impact on the overall shear resistance of a strata layer. The presence of moisture in these clayey materials can result in excess pore pressure when the rock stress increases and in reduced apparent friction angles. Field observations have shown that lateral sliding between beds can occur up to about 150 m (492 ft) ahead of a longwall face, which can partly be explained by the presence of low friction glide planes within the rock (Listak et al., 1987). When modeling the large-scale rock mass, it is necessary to include the effect of these weak planes in the rock mass strength.

Gob Properties

The subsidence profile is useful for calibrating the gob compaction characteristics. The maximum subsidence over a super-critical panel (panel width exceeds 1.2 times the panel depth) can be used to verify the gob compaction assumptions. When a panel is super-critical, the full overburden weight is carried by the gob, and the resulting subsidence is directly related to gob compaction characteristics. The SDPS subsidence prediction software (Newman et al., 2001) was initially used to create a suite of subsidence curves for various super-critical longwall geometries and geologies. Final verification was done by modeling published field trials and comparing the model results to actual subsidence measurements.

It was found that the gob compaction characteristics depend on the type of rock material in the gob. Gob that consists of the stronger rock types is less compressible than the weaker gob materials. To assist in selecting the appropriate gob parameters, an approach similar to that followed by the authors of the SDPS software was followed, in which the gob is characterized by the ratio of the thickness of "strong" to "weak" rocks in the overburden. Weak rocks include shales and claystones that have a uniaxial compressive strength of less than about 40 MPa (5,802 psi), while limestone, sandstones, and siltstones with strengths above 40 MPa (5,802 psi) would be classified as strong rocks. Figure 6 shows the stress-strain behavior of the various gob materials used in the models. The figure shows that the laboratory-

determined curves fall within the range of curves used in the models. Interestingly, the strong rock gob curve derived from full-scale subsidence is almost identical to the laboratory-determined curve for sandstone materials. Table 2 summarizes parameters for describing the gob curves using Equation 3 as used in the models.

Table 2. Parameters for modeling various gob types using Equation 3.

Overburden type	Ratio of strong: weak rocks	a parameter (MPa)	b parameter
Weak	25%	5.9	0.44
Moderate	35%	8.6	0.44
Strong	50%	12.8	0.44
Very strong	65%	25.2	0.44

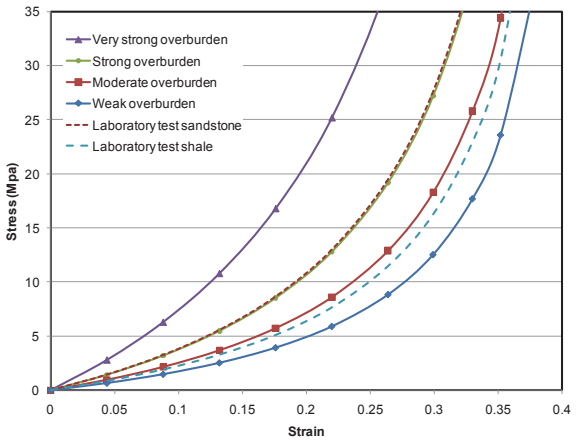

Figure 6. Stress-strain curves for gob materials determined through model calibration and results of laboratory tests on gob materials, after Pappas and Mark (1998).

VERIFICATION OF CALIBRATED MODELS

After completing the calibration exercises, a number of the case histories that were used for calibration were re-evaluated using the final set of input parameters and modeling technique. Three examples are presented here showing a variety of longwall mining and pillar extraction scenarios. The first example shows stress and subsidence results for a supercritical longwall panel under relatively weak overburden strata, typical of the Northern Appalachian coal fields. The second is a sub-critical longwall panel under strong strata found in the western United States. The third compares monitoring of pillar stress adjacent to a longwall with strong overburden strata.

Supercritical Longwall Panel

The first model simulates a longwall in the Pittsburgh seam where detailed subsidence measurements have been made (Zimmerman and Fritschen, 2007). The depth of cover is 180 m (591 ft) and the panel width is 350 m (1,148 ft) with a three-entry gate road system. The chain pillars were 24-m (79 ft) wide and the mining height was 1.7 m (5.6 ft).

The chain pillars, the solid abutments, and the gob were modeled using the equivalent pillar approach (Esterhuizen and Mark, 2009) in which model elements are prescribed to follow the stress-strain relationships of the pillars, gob, and abutment edges. The pillars were specified to follow the stress-strain relationships derived from numerical models, using the approach described in this paper. The gob was modeled as a weak material associated with 25% strong overburden, using the parameters listed in Table 2. The overburden in this area consists of alternating layers of shale, siltstone, sandstone, and limestone. The limestone is typically strong and massive with poorly developed bedding planes. The limestone was modeled without any weak bedding planes, but vertical joints were included. The extraction of the longwall was modeled by extracting the coal elements and replacing them with gob elements and allowing the overburden to settle onto the gob. The model results were evaluated against the measured surface subsidence and empirical predictions of the likely extent of the abutment stress and the stress distribution in the chain pillars.

The subsidence results are presented in Figure 7, which shows that excellent agreement is achieved between the vertical displacements in the model and subsidence measurements. This confirms that the gob compaction curve is realistic, since the maximum subsidence agrees with observations. In addition, the curvature of the overburden at the edges of the subsidence trough and the location of the subsidence trough relative to the edge of the longwall panel are satisfactory. This indicates that the large-scale stiffness and deformation of the overburden is modeled with sufficient accuracy.

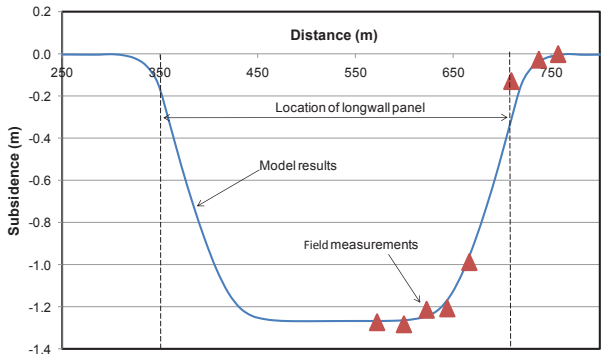

Figure 7. Comparison of model subsidence results and field measurements for a supercritical panel in the Pittsburgh coal bed. Subsidence measurements after Zimmerman and Fritschen (2007).

The stress distribution on the mining horizon, determined from the model results and from the Mark's (1987) empirical equation is shown in Figure 8. The columns showing the model results are 12-m (39-ft) wide, representing the width of the elements. The results show that the extent of the abutment zone extends about 72 m (236 ft) away from the edge of the gob, which is the same as the value predicted by the empirical equation of Peng and Chiang (1984). The empirical curve predicts the average stress on the 24-m-wide chain pillar marked 'A' in Figure 8 to be 23.6 MPa (3,422.9 psi) while the model result is 22.7 MPa (3,292.4 psi), which is a satisfactory outcome. The results for the second chain

pillar, marked 'B' in Figure 8, differ by a greater amount; mainly because the empirical equation does not take into account the fact that this pillar is adjacent to the stiffer unmined abutment and assumes the pillar carries the full tributary loading.

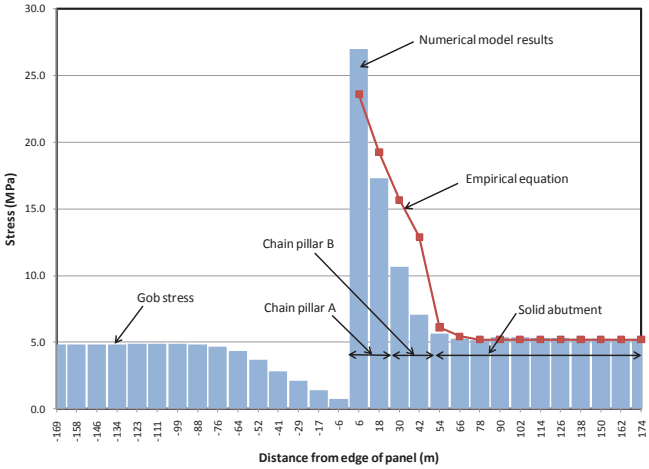

Figure 8. Comparison of empirical and numerical model derived stress distribution on the seam level for a 350 m (1,150 ft) wide longwall at 180 m (600 ft) depth of cover in the Pittsburgh coal bed.

The results show that for this test case, the developed input parameters for modeling the coal pillar, overburden and gob performed very satisfactorily against the measured subsidence and expected stress distributions on the coal seam.

Subsidence Over a Sub-Critical Longwall Panel

The second example shows numerical model results for a longwall in strong overburden in central Utah. The subsidence was measured during the mining of a number of longwall panels (Allgaier, 1988). The average depth of cover was about 450 m (1,476 ft) and the average mining height was 3 m (10 ft) in the Blind Canyon coal bed. The subsidence related to the first two panels, panel 5E and 6E, of a series of four longwall panels was selected for analysis. The panel widths were 146 and 164 m (479 and 538 ft) for the 5E and 6E panels respectively. The panels were separated by two rows of small chain pillars that had a width-to-height ratio of 3.2 and are considered to be yield pillars. The general geology is described as sandstones in thick beds and sandstone interbedded with siltstone. It is estimated that 45% of the overburden consists of sandstone.

Subsidence monitoring revealed vertical displacements of only about 60 mm (2.4 in) after mining the first panel as shown in Figure 9. The panel width-to-depth ratio was 0.32, which is highly sub-critical; therefore, the subsidence probably only reflected the elastic deflection of the strata. After mining the second panel, a subsidence trough developed with a maximum subsidence of just over 1.0 m (3.3 ft) that was centered over the first panel (see Figure 9). The location of the yield pillars between the two panels was not visible in the subsidence curve. The width-to-depth ratio of the two panels and the intervening yield pillars was 0.75, which is still sub-critical.

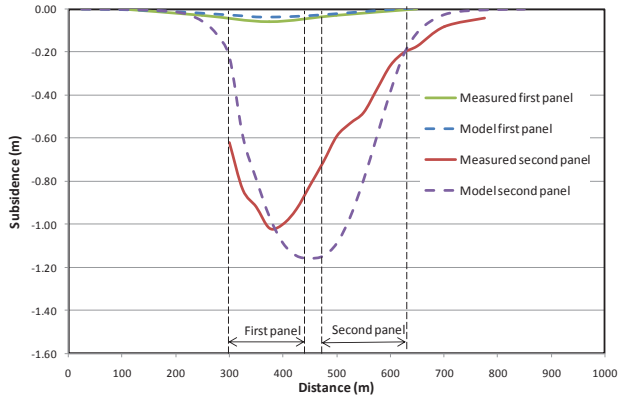

Figure 9. Comparison of model subsidence results and field measurements for two subcritical panels in a Utah coal mine. Subsidence measurements after Allgaier (1988).

The two longwalls and the overburden geology were modeled by simulating the published geologic profile using the calibrated set of input parameters for the overburden and gob. Sandstone strengths were set at 100 MPa (14,504 psi) and interbedded siltstone and sandstone materials were modeled with strengths between 60 MPa (702 psi) and 80 MPa (11,603 psi). The longwall extraction was modeled in stages with the coal being removed and replaced by strong gob properties, shown in Table 2. Subsidence results were obtained after mining of the first panel and the second panel. The results are also presented in Figure 9, which shows that for first-panel mining, the model results are very similar to the field measurements. The displacements are small, reflecting elastic displacement of the ground surface. Overburden failure and shearing along bedding planes was limited to the lower half of the model, with the upper rocks being undisturbed in terms of shearing or failure. After mining the second panel, the failure progressed up to the ground surface and the subsidence increased considerably, to a maximum of 1.16 m (3.81 ft), nearly symmetrically located over the mined area. The subsidence profile in the model also shows no sign of the yield pillars between the two panels, similar to the measurements.

The shape of the subsidence curve is satisfactory from the point of view of providing a reasonable agreement with the extent and maximum subsidence. More importantly, however, the modeled overburden responded correctly by arching over the first panel, resulting in negligible subsidence, and then subsiding to about 1 m (3.3 ft) when the second panel was extracted. This outcome demonstrates that the overburden modeling approach is reasonable, and it is able to capture the initial arching of the strata over the first panel, followed by the failure of the arch when the second panel was mined.

Pillar Stress Case Study in Strong Rock

The third case study presents a comparison of numerical model results to in-mine stress measurements in strong overburden strata. The stress changes, cable bolt performance, and entry deformations were monitored in a yield-abutment pillar system in the Hiawatha seam at the Crandall Canyon mine in Utah (Koehler et al., 1996). Two longwall panels at depths of cover of 396 m to 457 m (1,299 to 1,499 ft) were separated by a 9.1- (30-ft) wide yield pillar and a 36.6-m-wide abutment pillar. The longwall panels were overlain by strong sandstone and siltstone with occasional thin shale bands.

The strength of the roof strata generally fall between 69 Mpa (10,008 psi) and 138 MPa (20,015 psi), and several less competent zones with strengths below 50 MPa (7,252 psi) were reported. Monitoring results showed that the peak abutment stress of 45-50 MPa (6,527-7,252 psi) was located very near the edge of the abutment pillar, and there was a rapid drop off over about half the abutment pillar width, unlike the gradual decay one would expect from the Mark's (1987) empirical equation.

A numerical model was created that simulated the mining of the two panels, again using the equivalent pillar approach to model the pillars adjacent to the panels. The gob was modeled using the strong rock parameters in Table 2, and the overburden was modeled using the higher strength rock types in Table 1, interspersed with thin bands of weaker materials. The massive Castlegate sandstone in the upper part of the geologic profile was also included in the model.

Figure 10 shows the stress distribution predicted by the model and measured underground after the first longwall had mined past the monitoring site by about 260 m (854 ft) and the pillar system was subject to side loading from the first gob. It can be seen that the measurements show a peak stress of 48 MPa (6,962 psi), which drops down very rapidly to less than 20 MPa (2,901 psi) within the 36-m (118 ft) wide abutment pillar. The model results show a similar pattern of high stress, an average of 34 MPa (4,931 psi) in the portion of the pillar nearest the gob, dropping down to 17 MPa (7,252 psi) away from the gob. The yield pillar in the model yielded to a greater degree than the observations. This might be explained by the fact that the coal in the model was assumed to have a uniaxial compressive strength of 20 MPa (2,901 psi), while laboratory tests indicated that the coal at this mine was likely to be about 30 MPa (4,351 psi). The model stress results for the solid abutment is similar to the measured results. It is interesting to note that the model shows a long tail to the stress decay, which can explain the fact that forward abutment pressures were identified by the monitoring instruments up to 87 m (285 ft) ahead of the longwall face.

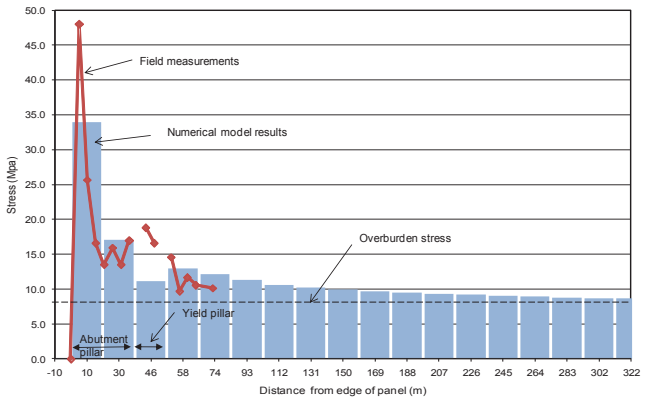

Figure 10. Comparison of numerical model results and field measurements of the stress at the edge of a longwall panel in the Western United States, after Koehler et al. (1996).

This case study shows that the model parameters can also provide satisfactory results for evaluating stress changes in longwall panels under stiff overburden. Although no subsidence data was available for this case, the model showed a dish shaped subsidence bowl forming over the two longwall panels, and the expression of the yield-abutment pillar system was not visible on the surface, which indicates that the strata were likely arching over the two panels.

The outcome of the third case study was again very satisfactory, showing that the input parameters and modeling approach is able to capture the stress distribution in both a weak rock scenario, shown in the first case study, as well as this strong rock scenario. The good agreement with measured stresses in the pillars is further verification that the numerical models are performing satisfactorily.

CONCLUSIONS

Modeling the large-scale response of coal measure rocks due to mining can be satisfactorily achieved using well-calibrated numerical models, provided the main characteristics of the coal pillars, the overburden, and the gob are captured in the models. This paper demonstrates how the FLAC3D software was used to obtain a base set of input parameters that can be used to evaluate the stress and deformation associated with mining in a variety of geological conditions, ranging from super-critical panels in weak overburden to sub-critical panels in strong rocks.

The calibration process described had the objective to obtain good agreement between model results and pillar strength, surface subsidence, and in-seam stress distributions. The models of individual pillars were calibrated against strong roof and floor case histories in which the pillar strength is governed by failure and yielding of the coal within the pillar and the strong surrounding strata had a limited impact on pillar strength. Subsidence matching assisted in verifying that the large-scale rock mass parameters and the gob compaction characteristics are realistic. Further calibration was carried out against stress measurements in coal pillars and in the unmined coal abutments. Good agreement was achieved between model results and actual measurements, which demonstrated that the interaction between the pillars and the surrounding strata was adequately captured in the models.

The paper provides a basic set of input data and a modeling approach that can be used for numerical modeling investigations of various coal mine designs using the FLAC3D software package. The models can be expected to provide realistic stress and deformation results, but further calibration would be required to determine the relationship between model results and actual mining conditions.

The model parameters presented are applicable for the FLAC3D software package. The parameters will be useful as initial estimates when using other modeling techniques, but each technique should be calibrated independently.

DISCLAIMER

The findings and conclusions in this paper have not been formally disseminated by the National Institute for Occupational Safety and Health and should not be construed to represent any agency determination or policy.

REFERENCES

Allgaier, F. K. (1988). Surface Subsidence Over Longwall Panels in the Western United States – Final Results at the Deer Creek Mine, Utah. U.S. Bureau of Mines IC 9194, 17 p.

Anon. (2007). Fast Lagrangian Analysis of Continua in 3 Dimension (FLAC-3D V3.1). Itasca Consulting Group, Minnesota.

Atkinson, R. H. and Ko, H. (1977). Strength Characteristics of U.S. Coals. Proceedings of the 18th U.S. Symposium on Rock Mechanics, Keystone, CO, pp. 2B3-1–2B3-6.

Barron, K. and Yang, T. (1992). Influence of Specimen Size and Shape on Strength of Coal. Proceedings of the Workshop in Coal Pillar Mechanics and Design, U.S. Bureau of Mines IC 9315, pp. 5–24.

Bieniawski, Z.T. (1968). The Effect of Specimen Size on the Strength of Coal. Int. J. Rock Mech. Min. Sci. *4*: 325–335.

Bieniawski, Z. T. (1992). A Method Revisited: Coal Pillar Strength Formula Based on Field Investigations. Proceedings of the Workshop in Coal Pillar Mechanics and Design, U.S. Bureau of Mines IC 9315, pp. 158–165.

Board, M. and Damjanac, B. (2003). Development of a Methodology for Analysis of Instability in Room and Pillar Mines. 2003 Swedish Rock Mechanics Day Conference, Ed. O. Stephansson, Stockholm: Svebefo, pp. 1–22.

Campoli, A. A., Barton, T. M., Van Dyke, F. C. and Gauna, M. (1990). Mitigating Destructive Longwall Bumps Through Conventional Gate Entry Design, U.S. Bureau of Mines RI 9325, 38 p.

Chugh, Y. P. and Pytel, W. M. (1992). Design of Partial Extraction Coal Mine Layouts for Weak Floor Strata Conditions. Proceedings of the Workshop in Coal Pillar Mechanics and Design, U.S. Bureau of Mines IC 9315, pp. 32–49.

Das, M.N. (1986). Influence of Width/Height Ratio on Post Failure Behavior of Coal. Int. J. Min. and Geol. Eng. *4*:79–97.

Dolinar, D. (2003). Variation of Horizontal Stresses and Strains in Mines in Bedded Deposits in the Eastern and Midwestern United States. Proceedings of the 22nd International Conference on Ground Control in Mining, pp. 178–185.

Esterhuizen, G. S. and Barczak, T. M. (2006). Development of Ground Response Curves for Longwall Tailgate Support Design. Proceedings of the 41st U.S. Rock Mechanics Symposium, Golden, CO, Paper 06-935.

Esterhuizen, G. S. and Mark, C. (2009). Three-Dimensional Modeling of Large Arrays of Pillars for Coal Mine Design. Proceedings of the International Workshop on Numerical Modeling for Underground Mine Excavation Design, Esterhuizen, Mark, Klemetti, Tuchman, eds., NIOSH IC 9512, pp. 37–46.

Gadde, M. M. (2009). Numerical Model Evaluation of Floor Bearing Capacity in Coal Mines. Proceedings of the International Workshop on Numerical Modeling for Underground Mine Excavation Design, NIOSH IC 9512, pp. 47–54.

Gadde, M., Rusnak, J., Honse, J. and Peng, S.S. (2007). On Rock Failure Criteria for Coal Measure Rocks. Proceedings of the 26th International Conference on Ground Control in Mining, pp. 361–369.

Gale, W. J. (1999). Experience of Field Measurement and Computer Simulation Methods of Pillar Design. Proceedings of the Second International Workshop on Coal Pillar Mechanics and Design, NIOSH IC 9448, pp. 49–61.

Hoek E., and Brown E. T. (1980). Underground Excavations in Rock. Inst. Min. Metallurgy, London, 527 p.

Hoek, E. and Brown, E. T. (1997). Practical Estimates of Rock Mass Strength. Int. J. Rock Mech. & Min. Sci. & Geomech., Abstr., *34*:1165–1186.

Hoek, E. T., Grabinsky, M. W., and Diederichs, M. S. (1990). Numerical Modelling for Underground Excavation Design. Trans Inst Min Metall., Section A: Mining Industry *100*:A22–A30.

Hoek, E., Carranza-Torres, C., and Corkum, B. (2002). Hoek-Brown Failure Criterion – 2002 Edition. Proceedings of the 5th North American Rock Mechanics Symposium, Toronto, pp. 267–273.

Iannacchione, A. T. (1990a). Behavior of a Coal Pillar Prone To Burst in the Southern Appalachian Basin of the United States. Rockburst and Seismicity in Mines, Balkema, Rotterdam, pp. 295–300.

Iannacchione, A.T. (1990b). The Effects of Roof and Floor Interface Slip on Coal Pillar Behavior. Rock Mechanics Contributions and Challenges, A. A. Balkema, Rotterdam, pp. 153–160.

Koehler, J., Demarco, M., Marshall, R., and Fielder, J. (1996). Performance Evaluation of a Cable Bolted Yield-Abutment Gate Road System at the Crandall Canyon No. 1 Mine, Genwall Resources, Inc., Huntington, Utah. Proceedings of the 15th International Conference on Ground Control in Mining, pp. 477–495.

Listak, J. M., Hill, J. L. and Zelanko, J. C. (1987). Characterization and Measurement of Longwall Rock Mass Movement. U.S. Bureau of Mines IC 9137, 26 p.

Lu J., Ray, A., Morsy, K. and Peng, S. S. (2008). Effects of Coal/Rock Interface Property on Coal Pillar Strength. Proceedings of the 27th International Conference on Ground Control in Mining, pp. 262–267.

Mark, C. (1987). Analysis of Longwall Pillar Stability. Ph.D. Thesis, Pennsylvania State University, 414 p.

Mark, C. and Chase, F. E. (1997). Analysis of Retreat Mining Pillar Stability. Proceedings of the New Technology for Ground Control in Retreat Mining, NIOSH IC 9446, pp. 17–34.

Mark, C. and Gadde, M. (2008). Global Trends in Coal Mine Horizontal Stress Measurements. Proceedings of the 27th International Conference on Ground Control in Mining, pp. 319–331.

Medhurst, T. P. and Brown, E. T. (1988). A Study of the Mechanical Behaviour of Coal for Pillar Design. Int. J. Rock Mech. Min. Sci. *35*:1087–1105.

Morsy, K. and Peng, S. S. (2001). Typical Complete Stress-Strain Curves of Coal. Proceedings of the 20th International Conference on Ground Control in Mining, pp. 210–217.

Newman, D. A. and Hoelle, J. L. (1993). The Impact of Variability in Coal Strength on Mine Planning and Design – A Case History. Proceedings of the 12th International Conference on Ground Control in Mining, pp. 237–243.

Newman, D. A., Agioutantis, Z. and Karmis, M. (2001). SDPS for Windows: An Integrated Approach to Ground Deformation Prediction. Proceedings of the 20th International Conference on Ground Control in Mining, pp. 157–162.

Oram J. (1996). An Investigation Into the Behavior of Yield Pillar Multi Entry System at JWR No. 7 Mine: Part 4. Unpublished Report By Rock Mechanics Technologies United Kingdom, 31 p.

Pappas, D. M. and Mark, C. (1993). Behavior of Simulated Gob Material. U.S. Bureau of Mines RI 9458.

Peng, S. S. and Chiang (1984). Longwall Mining, Wiley, New York.

Rusnak, J. and Mark, C. (2000). Using the Point Load Test To Determine the Uniaxial Compressive Strength of Coal Measure Rock. Proceedings of the 19th International Conference on Ground Control in Mining, pp. 362–371.

Salamon M. D. G. and Wagner H. (1985). Practical Experiences in the Design of Coal Pillars. Proceedings of the 21st International Conference of Safety in Mines Research Institutes, Sydney, Australia, pp. 3–10.

Salamon M. D. G. (1990). Mechanism of Caving in Longwall Coal Mining. Proceedings of the 31st U.S. Rock Mechanics Symposium, Denver CO, A. A. Balkema, pp. 161–168.

Skiles, M. and Stricklin, K. (2009). General Guidelines for the Use of Numerical Modeling to Evaluate Ground Control Aspects of Proposed Coal Mining Plans. Washington, D.C.: Mine Safety and Health Administration, Program Information Bulletin No. P09-03, Issue Date: March 16, 2009, 7 p.

Wang, Q. and Heasley K. (2005). Stability Mapping System. Proceedings of the 24th International Conference on Ground Control in Mining, pp. 243–249.

Wilson, A. H. (1972). A Hypothesis Concerning Pillar Stability. The Mining Engineer *131*:409–417.

Zimmerman, K. and Fritschen, R. (2007). Study About the Dynamic Influence of Longwall Mining in the U.S. on Surface Structures. Proceedings of the 26th International Conference on Ground Control in Mining, pp. 79–84.

Zipf R. K. (2007). Numerical Modeling Procedures for Practical Coal Mine Design. Proceedings of the International Workshop on Rock Mass Classification in Underground Mine Design, NIOSH IC 9498, pp. 153–162.

Zoback, M. L. and Zoback, M. D. (1989). Tectonic Stress Field of the Continental United States. Geol. Soc. of American Memoir 172, pp. 523–539.